NURETH14-226

ONSET OF STABLE DRYOUT CONDITION IN DIABATIC ANNULAR TWO-PHASE FLOW

H. Anglart

Royal Institute of Technology (KTH), Stockholm, Sweden

Abstract

Conditions for the formation of a stable dry patch in vertical diabatic annular two-phase flows are investigated. An analytical model of the force balance for the leading edge of the liquid film is developed. In addition to surface tension, evaporation thrust and capillary forces, the model includes the effect of turbulence, the pressure gradient and the interfacial shear stress. Numerical evaluations are performed to validate the model and to indicate the importance of various factors on the dry patch stability and on the resulting minimum wetting rate of the liquid film. The analyses indicate that good agreement with measurements is obtained in case of stagnant patch formed on liquid film flowing down a vertical surface.

Introduction

The critical heat flux (CHF) is one of the major design limiting factors in high performance heat exchangers encountered in many industrial applications such as cooling systems of electronic devices, steam generators and fuel assemblies of nuclear reactors. In high quality two-phase flows, when the annular flow pattern prevails, the CHF occurs when the liquid film dries out and a permanent dry patch is formed. For that reason this type of CHF is often termed as dryout. Even though the dryout mechanism is quite well understood, there is still lack of a consistent theory that is capable to predict the occurrence of dryout in arbitrary geometry and under any flow conditions. Due to that high precision predictions which are required in the safety evaluations of nuclear reactors still rely on correlations derived from full scale experiments.

The key issue in prediction of the occurrence of dryout in annular two-phase flows is to ascertain conditions that are necessary for creation of a permanent dry patch. The dry patch may appear, of course, due to a complete evaporation of the liquid film. This hypothesis is a basis of several existing phenomenological models, which use the mass balance equation for the liquid film to predict the location of the dry patch in places where the film completely disappears, [1], [2]. There are, however, experimental evidences that dryout occurs even when the mass flow rate in the liquid film per unit perimeter is as high as 0.8 kg/m.s, [3]. This so called critical film flow rate is virtually equal to zero when the flow quality is higher than 50 %, but it rapidly increases when the quality decreases below that value. Thus, it seems plausible to argue that for the occurrence of dryout it is necessary that: (a) the liquid film attains a minimum or "critical" flow rate at which the film breaks down, (b) a stable dry patch is created. The former may occur either spontaneously or due to presence of disturbances in the liquid film. It should be noted that if only condition (a) is satisfied no dryout will occur. Fukano et al. [4] performed dryout experiments in channels with obstacles and reported that close to CHF the heating surface was repeatedly dried out by evaporation of the liquid film and rewetted by the passing of disturbance waves. A stable dry patch was created and an onset of dryout was noted only after further increase of the heat flux.

The minimum stable film flow rate has been extensively investigated by several researches. Hobler [5] proposed a theory where the minimum wetting rate of a film flowing down a vertical wall was derived from the minimum condition of the total energy of the liquid film. This approach has been subsequently employed and extended by e.g. Bankoff [6], Mikielewicz and Moszynski [7], Doniec [8], El-Genk and Saber [9] and Mikielewicz et al. [10].

There are reasons to believe that the minimum stable film flow rate, as predicted by the total energy theory, is not applicable to CHF conditions in annular two-phase flows. Hewitt and Lacey [11] investigated the breakdown of the liquid film in annular air-water two phase flow. Their experiments indicate that films can exist in meta-stable state and will not break down unless there is an external disturbance. The spontaneous breakdown of the film typically occurs at very low film mass flow rates. However, when a disturbance is present, the film breakdown occurs at much higher film flow rates, resulting from the stability condition of the liquid film motion. Such effects as nucleation, Marangoni forces and evaporation on the interface may de-stabilize the liquid film and cause its premature breakdown.

The objective of the current analysis is to investigate the conditions under which a stable dry patch can exists in annular two-phase flow. The previous analyses by Hartley and Murgatroyd [12], as well as by Zuber and Staub [13] are extended to include the effects of the turbulence, the pressure gradient and the interfacial shear stress.

1. The model formulation

Various models have been developed for prediction of the stable condition of a dry patch. Hartely and Murgatroyd [12] proposed to employ the force balance to predict a stagnation condition of the dry patch. The same approach has been later used by Zuber and Staub [13] and McPherson [14], who added additional effects to the force balance such as resulting from the thermo-capillary, vapor thrust and drag forces.

The present approach enlarges on the ideas of the above cited work and includes the following new aspects:

- vertical climbing film on a heated wall,
- pressure drop in the channel and the interfacial shear stress,
- turbulent liquid film flow.

A stable dry patch in the liquid film will be formed when all forces acting on the leading edge of the liquid film are in balance. In the present model, the following forces are taken into consideration:

- the stagnation pressure force,
- the surface tension force,
- the thermo-capillary force,

- the vapor thrust force,
- the skin and the shape drag force.

Figure 1 shows the assumed geometry of the leading edge of the liquid film flowing vertically up in a heated channel. A uniform film of an average thickness δ_c and velocity w approaches the leading edge between points A and C. The shape of the leading edge depends on the surface as well as on the hydrodynamic forces. At point A, a stable vertex of the dry patch is formed. As the liquid film approaches this vertex, flow separates into rivulets which are formed on both sides of the dry patch.

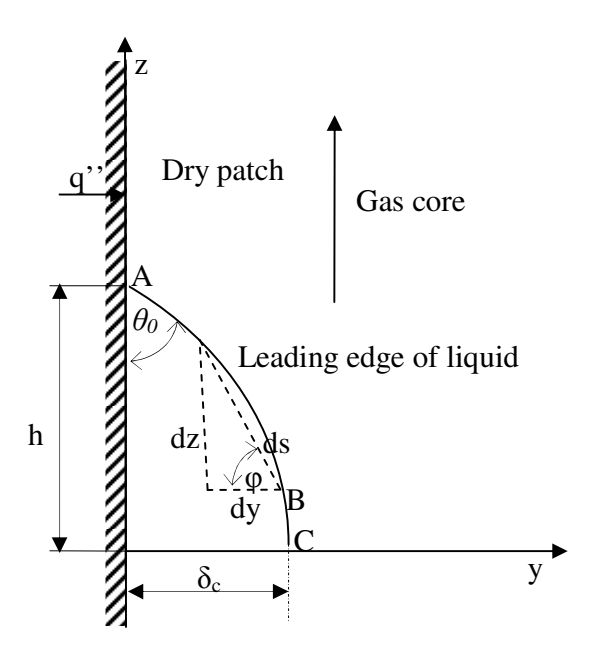


Figure 1 A leading edge of a liquid film upstream of a dry patch.

The interface of the leading edge is making an angle θ_0 with the wall surface, which is equal to the contact angle at the prevailing local conditions. The height of the leading edge h is equal to a distance from point C, where the stable film exists to point A, where the stable dry patch vertex is formed. At any point B located at the interface between points A and C, the shape of the leading edge is characterized by an angle φ that a tangential to the interface makes with a line perpendicular to the wall surface. In the following, the forces acting on the leading edge of the liquid film will be expressed in terms of the above mentioned parameters.

1.1 The velocity profile

For shear-driven laminar flow in the liquid film, the velocity distribution is obtained from a solution of the following differential equation, describing the momentum conservation in the film,

$$-\frac{\partial p}{\partial z} + \mu_l \frac{d^2 w}{dy^2} + \rho_l g_z = 0, \tag{1}$$

with the following boundary conditions,

$$y = 0 \Rightarrow w = 0$$
 and $y = \delta \Rightarrow \mu_i \frac{dw}{dy} = \tau_i$ (2-3)

The solution of Eqs. (1-3) is as follows,

$$w(y) = -\frac{\left(-\frac{\partial p}{\partial z} + \rho_l g_z\right) \delta^2}{2\mu_l} \left[\left(\frac{y}{\delta}\right)^2 - 2\frac{y}{\delta} \right] + \frac{\tau_i}{\mu_l} y. \tag{4}$$

In case of turbulent flow in the liquid film, the momentum equation and the boundary conditions are as follows.

$$-\frac{\partial p}{\partial z} + \frac{d}{dy} \left(\mu_{eff} \frac{dw}{dy} \right) + \rho_l g_z = 0, \tag{5}$$

$$y = 0 \Rightarrow w = 0 \text{ and } y = \delta \Rightarrow \mu_{eff} \frac{dw}{dy} = \tau_i$$
 (6-7)

Here μ_{eff} is the effective dynamic viscosity, which is a sum of the molecular dynamic viscosity and the eddy viscosity. Various models can be applied to calculate this quantity. In general, the eddy viscosity in liquid films is evaluated using relations that have been developed for turbulent flows in tubes. However, such models are not correct close to the liquid film interface, where the turbulence damping is observed. In the present approach, the influence of the turbulence model is simulated by employing three different formulations: the mixing length model, the modified mixing length model with interface damping and the eddy viscosity model proposed by Blanghetti and Schlunder [15].

Employing the standard mixing length model, the effective viscosity is obtained as,

$$\mu_{eff} = \mu_l + \rho_l \kappa^2 y^2 \left| \frac{dw}{dy} \right|, \tag{8}$$

where κ is the von Karman constant. In the modified mixing length approach, the damping at the interface is introduced as follows,

$$\mu_{eff} = \begin{cases} \mu_l + \rho_l \kappa^2 y^2 \left| \frac{dw}{dy} \right| & 0 \le y \le \delta/2 \\ \mu_l + \rho_l \kappa^2 (y - \delta)^2 \left| \frac{dw}{dy} \right| & \delta/2 < y \le \delta \end{cases}$$

$$(9)$$

In the Blanghetti and Schlunder model, the effective viscosity is found as,

$$\mu_{eff} = \min(\mu_{eff1}, \mu_{eff2}), \tag{10}$$

where

$$\mu_{eff1} = 0.5\mu_{l} \left\{ 1 + \left[1 + 0.64y^{+2} \left(1 - e^{-y^{+2}/26} \right) \right]^{1/2} \right\},\tag{11}$$

$$\mu_{eff 2} = \mu_{l} \left\{ 1 + \frac{0.0161 \text{Ka}^{1/3} \text{Re}_{l}^{1.34}}{\left(v_{l}^{2}/g\right)^{1/3}} \left[\frac{\tau}{g(\rho_{l} - \rho_{v})} + \delta \left(1 - \frac{y^{+}}{\delta^{+}}\right) \right] \left(\delta^{+} - y^{+}\right) \right\}.$$
(12)

Here the following dimensionless numbers are used,

$$Ka = \frac{\rho_l^3 g^3 (v_l^2 / g)^{1/3}}{\sigma}$$
 and $Re_l = \frac{4\Gamma}{\mu_l}$. (13-14)

The liquid film Reynolds number, Re_l , is defined in terms of the film mass flow rate per unit wetted perimeter, Γ , obtained as follows,

$$\Gamma = \rho_l \int_0^\delta w(y) dy \tag{15}$$

The shear stress $\tau(y)$ in Eq. (12) is given as,

$$\tau(y) = \tau_i - \left(\frac{\partial p}{\partial z} + \rho_l g\right) (\delta - y), \tag{16}$$

and the dimensionless distance to the wall, y^+ , as well as the dimensionless film thickness, δ^+ , are defined as,

$$y^{+} = \frac{(\tau_{w}/\rho)^{1/2} y}{v_{I}}$$
 and $\delta^{+} = \frac{(\tau_{w}/\rho)^{1/2} \delta}{v_{I}}$. (17-18)

The velocity distribution in the liquid film, w(y), is obtained from a numerical integration of Eq. (5) with boundary conditions (6-7) and with the effective viscosity, μ_{eff} , determined by Eqs. (8-18). Both the stagnation force and the film flow rate are obtained numerically as well.

1.2 The stagnation force

The stagnation force per unit film perimeter acting in z-direction is given as follows,

$$F_{spz} = \frac{\rho_l}{2} \int_0^{\delta_c} w^2(y) dy. \tag{19}$$

Here $\delta = \delta_c$ is the critical film thickness at point C shown in Fig. 1. For shear-driven laminar flow, the force can be obtained analytically and is as follows,

$$F_{spz} = \frac{\rho_l}{15} \left(\frac{-\frac{\partial p}{\partial z} + \rho_l g_z}{\mu_l} \right)^2 \delta_c^5 + \frac{5\rho_l \left(-\frac{\partial p}{\partial z} + \rho_l g_z \right) \tau_i}{24\mu_l^2} \delta_c^4 + \frac{\rho_l \tau_i^2}{6\mu_l^2} \delta_c^3.$$
 (20)

In case of turbulent flow a numerical integration is necessary, using the velocity profile obtained from a numerical solution of Eqs. (5-7) with the effective viscosity given be Eqs. (8-18).

1.3 The surface tension force

The surface tension force acting in z-direction is given as follows,

$$F_{stz} = \sigma_A \cos \theta_0 - \sigma_C, \tag{21}$$

where θ_0 is the contact angle and σ_A and σ_C is the surface tension at points A and C, as shown in Fig. 1. Taking into account the temperature variation of the surface tension, the surface tension at point C can be expressed in terms of the surface tension at point A as follows,

$$\sigma_C = \sigma_A + \int_A^C \frac{\partial \sigma}{\partial s} ds = \sigma_A + \int_A^C \frac{\partial \sigma}{\partial T} \frac{\partial T}{\partial y} \frac{\partial y}{\partial s} ds = \sigma_A - \int_A^C \frac{\partial \sigma}{\partial T} \frac{q''}{\lambda_l} \cos \phi ds.$$
 (22)

Thus, combining Eqs. (21) and (22), the surface tension force becomes,

$$F_{stz} = \sigma_A (\cos \theta_0 - 1) + \int_A^C \frac{\partial \sigma}{\partial T} \frac{q''}{\lambda_t} \cos \phi ds . \tag{23}$$

1.4 The thermo-capillary force

Due to heating the temperature of the interface may not be constant and a shear stress will be generated as follows,

$$\tau_{tc} = \frac{\partial \sigma}{\partial s} \,. \tag{24}$$

Here s is the linear coordinate along the interface of the leading edge. The differential thermocapillary force acting on segment ds and projected onto z-direction is as follows,

$$dF_{tcz} = -dF_{tc}\sin\phi = -\frac{\partial\sigma}{\partial s}\sin\phi ds. \tag{25}$$

Thus, the z-component of this force is obtained as,

$$F_{tcz} = -\int_{A}^{C} \frac{\partial \sigma}{\partial s} \sin \phi ds.$$
 (26)

1.5 The vapor thrust force

The net vapor thrust per unit perimeter and per a differential length of the interface ds is as follows,

$$dF_{vt} = \gamma''(v_{vn} - v_{ln})ds, (27)$$

where γ'' is the evaporation rate per unit interface area and v_{vn} and v_{ln} are vapor and liquid velocities normal to the interface, respectively. Mass conservation on the interface yields, $\gamma'' = \rho_l v_{ln} = \rho_v v_{vn}$, and since, $v_{ln} = \rho_v v_{vn}/\rho_l$, the vapor thrust force projected onto z-direction becomes,

$$F_{vtz} = \int_{A}^{C} \gamma'' (v_{vn} - v_{ln}) \cos \phi ds = \int_{A}^{C} \rho_{v} v_{vn}^{2} \left(1 - \frac{\rho_{v}}{\rho_{l}} \right) \cos \phi ds . \tag{28}$$

The evaporation rate can be obtained from the energy balance as follows,

 $q''dz = \gamma''i_{fg}ds = \rho_v v_{vn}i_{fg}ds$. This equation can be written as $v_{vn} = q''dz/\rho_v i_{fg}ds = q''\sin\phi/\rho_v i_{fg}$. Combining the two last expressions and substituting into Eq. (28) yields,

$$F_{vtz} = \int_{A}^{C} \rho_{v} \left(\frac{q''}{\rho_{v} i_{fg}} \right)^{2} \left(1 - \frac{\rho_{v}}{\rho_{t}} \right) \sin^{2} \phi \cos \phi ds.$$
 (29)

1.6 The drag force

The total skin drag force acting in z-direction is obtained as,

$$F_{sdz} = -\int_{A}^{C} \tau_{i} \sin \phi ds . \tag{30}$$

Here τ_i is the interfacial shear stress. The total form drag force projected onto z-axis is as follows,

$$F_{fdz} = -\int_{A}^{C} p_{vi} \cos \phi ds \,. \tag{31}$$

Here p_{vi} is the vapor pressure at the interface.

The form drag force results from the pressure distribution along the leading edge of the liquid film. The vapor pressure distribution is approximated as,

$$p_{vi} = p_{vC} + \left(\frac{\partial p}{\partial z}\right)_C (z - z_C), \tag{32}$$

where $\left(\frac{\partial p}{\partial z}\right)_C$ is the total pressure gradient in z-direction in the channel at location C. In writing Eq.

(32) it is assumed that the pressure in the gas core changes linearly with the pressure gradient evaluated at point C. Thus, the form drag force is as follows,

$$F_{fdz} = -\int_{A}^{C} \left[p_{vC} + \left(\frac{\partial p}{\partial z} \right)_{C} (z - z_{C}) \right] \cos \phi ds =$$

$$-\int_{A}^{C} \left(\frac{\partial p}{\partial z} \right)_{C} (z - z_{C}) \cos \phi ds = -\left(\frac{\partial p}{\partial z} \right)_{C} \int_{C}^{C} (z - z_{C}) \cos \phi ds$$

$$(33)$$

2. The force balance

The formulation of the force balance requires the information on the shape of the interface along the leading edge of the liquid film, which, in principle, is a part of the solution. Strictly speaking this shape can be obtained from a solution of the Laplace relationship between the pressure difference over the interface and the interface curvature. However, it is expected that the results of such analysis would heavily depend on the assumed pressure distributions along the interface. Since these pressure distributions are not well determined, it is thus justified to employ an approximation in which the radius of the curvature of the interface results from the contact angle and the critical film thickness, as shown in Fig. 2. An additional advantage of the present approximation is that an analytical expression for the force balance can be obtained which is necessary to discern the importance of various effects.

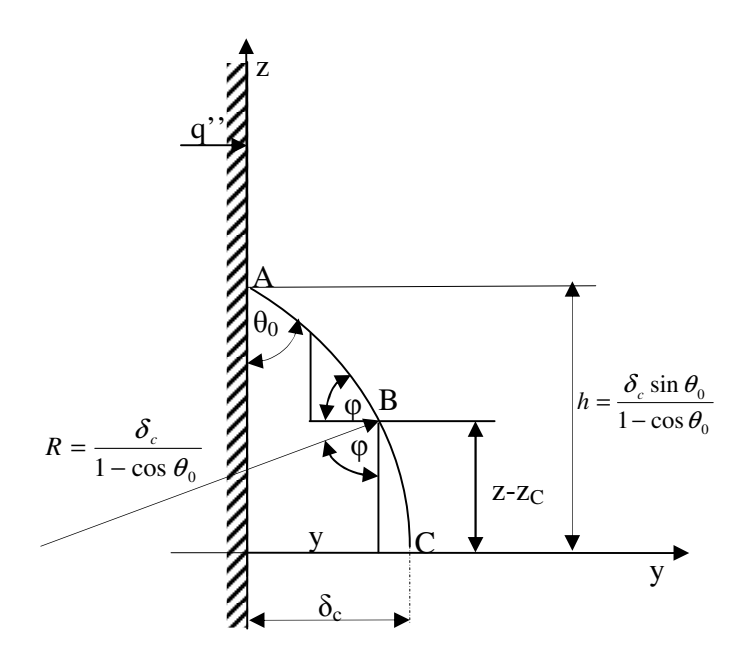


Fig. 2. Assumed curvature of the leading edge of the liquid film.

With this assumption, the forces are as follows:

- the stagnation force is given by Eq. (20) and it doesn't depend on the shape of the leading edge of the liquid film,
- the surface tension force, Eq. (23), depends on the shape of the leading edge and becomes,

$$F_{stz} = \sigma_A \left(\cos \theta_0 - 1\right) + \frac{\partial \sigma}{\partial T} \frac{q''}{\lambda_i} \delta_c, \tag{23a}$$

- the thermo-capillary force, Eq. (26), is as follows,

$$F_{lcz} = \frac{d\sigma}{dT} \frac{q''}{\lambda_l} \frac{\delta_c}{2} (1 + \cos\theta_0), \tag{26a}$$

- the vapor thrust force, Eq. (29), becomes,

$$F_{vtz} = \rho_v \left(\frac{q''}{\rho_v i_{fg}} \right)^2 \left(1 - \frac{\rho_v}{\rho_l} \right) \frac{\delta_c}{3} \left(1 + \cos \theta_0 + \cos^2 \theta_0 \right), \tag{29a}$$

- the skin drag force, Eq. (30), is as follows,

$$F_{sdz} = \frac{\tau_i \delta_c \sin \theta_0}{1 - \cos \theta_0}, \tag{30a}$$

- the form drag, Eq. (33), becomes,

$$F_{fdz} = -\left(\frac{\partial p}{\partial z}\right)_C \frac{1}{2(1-\cos\theta_0)^2} \left[\theta_0 - \cos\theta_0 \sin\theta_0\right] \delta_c^2. \tag{33a}$$

The force balance for the leading edge of the liquid film is as follows,

$$F_{spz} + F_{stz} + F_{tcz} + F_{vtz} + F_{sdz} + F_{fdz} = 0 (34)$$

In case of laminar flow, the force balance can be written explicitly in terms of the critical film thickness by substituting Eqs. (20), (23a), (26a), (29a), (30a) and (33a) into (34) as follows,

$$\frac{\rho_{l}}{15} \left(\frac{-\frac{\partial p}{\partial z} + \rho_{l} g_{z}}{\mu_{l}} \right)^{2} \delta_{c}^{5} + \frac{5\rho_{l} \left(-\frac{\partial p}{\partial z} + \rho_{l} g_{z} \right) \tau_{i}}{24\mu_{l}^{2}} \delta_{c}^{4} + \frac{\rho_{l} \tau_{i}^{2}}{6\mu_{l}^{2}} \delta_{c}^{3} - \left(\frac{\partial p}{\partial z} \right)_{c} \frac{1}{2(1 - \cos\theta_{0})^{2}} \left[\theta_{0} - \cos\theta_{0} \sin\theta_{0} \right] \delta_{c}^{2} + \left(\frac{\partial \sigma}{\partial T} \frac{q''}{\lambda_{l}} \frac{(1 - \cos\theta_{0})}{2} - \rho_{v} \left(\frac{q''}{\rho_{v} i_{fg}} \right)^{2} \left(\frac{\Delta \rho}{\rho_{l}} \right) \frac{(1 + \cos\theta_{0} + \cos^{2}\theta_{0})}{3} + \frac{\tau_{i} \sin\theta_{0}}{1 - \cos\theta_{0}} \right] \delta_{c} + \sigma(\cos\theta_{0} - 1) = 0$$
(34a)

For shear-driven turbulent flow in the liquid film, the force balance is obtained by substituting Eqs. (19), (23a), (26a), (29a), (30a) and (33a) into (34) as follows,

$$\frac{\rho_{l}}{2} \int_{0}^{\delta_{c}} w^{2}(y) dy - \left(\frac{\partial p}{\partial z}\right)_{c} \frac{1}{2(1 - \cos\theta_{0})^{2}} \left[\theta_{0} - \cos\theta_{0}\sin\theta_{0}\right] \delta_{c}^{2} + \left[\frac{\partial \sigma}{\partial T} \frac{q''}{\lambda_{l}} \frac{(1 - \cos\theta_{0})}{2} - \rho_{v} \left(\frac{q''}{\rho_{v} i_{fg}}\right)^{2} \left(\frac{\Delta \rho}{\rho_{l}}\right) \frac{(1 + \cos\theta_{0} + \cos^{2}\theta_{0})}{3} + \frac{\tau_{i} \sin\theta_{0}}{1 - \cos\theta_{0}}\right] \delta_{c} + .$$

$$\sigma(\cos\theta_{0} - 1) = 0$$
(34b)

Equation (34a) is a polynomial of 5-th degree that describes the dry patch stagnation condition in annular two-phase flow with heating. The real and positive root of the polynomial gives the minimum, or critical, film thickness at which the dry patch will remain stable. Correspondingly, Eq. (34b) can be solved iteratively to obtain the value of the minimum film thickness in case of the turbulent flow in the liquid film. A comparison of predictions with experimental data and a significance of various effects and their influence on the minimum film thickness are presented in the next sections.

3. Model validation

The model given by Eq. (34a) has been compared with available measured data and with selected analytical models. The experimental data with measured minimum film thickness for vertical boiling two-phase annular up-flow could not be found. Most of the data are obtained for adiabatic liquid films flowing down [16], [17]. Hewitt and Lacey [11] measured the minimum wetting rate for a climbing film, in which a dry patch was created by blowing air. It should be mentions that the accuracy of prediction of the minimum wetting rate strongly depends on the accuracy of the corresponding contact angle used in calculations. In most cases the equilibrium contact angle is measured, whereas very little is known about the dynamic contact angle, in particular at the leading edge of liquid film with evaporation. Ponter et al. [17] measured the minimum wetting rate for liquid films flowing down on stainless steel, copper and Perspex surfaces. They also provide data for the equilibrium contact angle for various temperatures and surface conditions. Figure 3 shows the predicted minimum wetting rate using Eq. (34a) in comparison with the measured data. Predictions obtained from models given by El-Genk and Saber [9] and Ponter et al. [16] are shown as well.

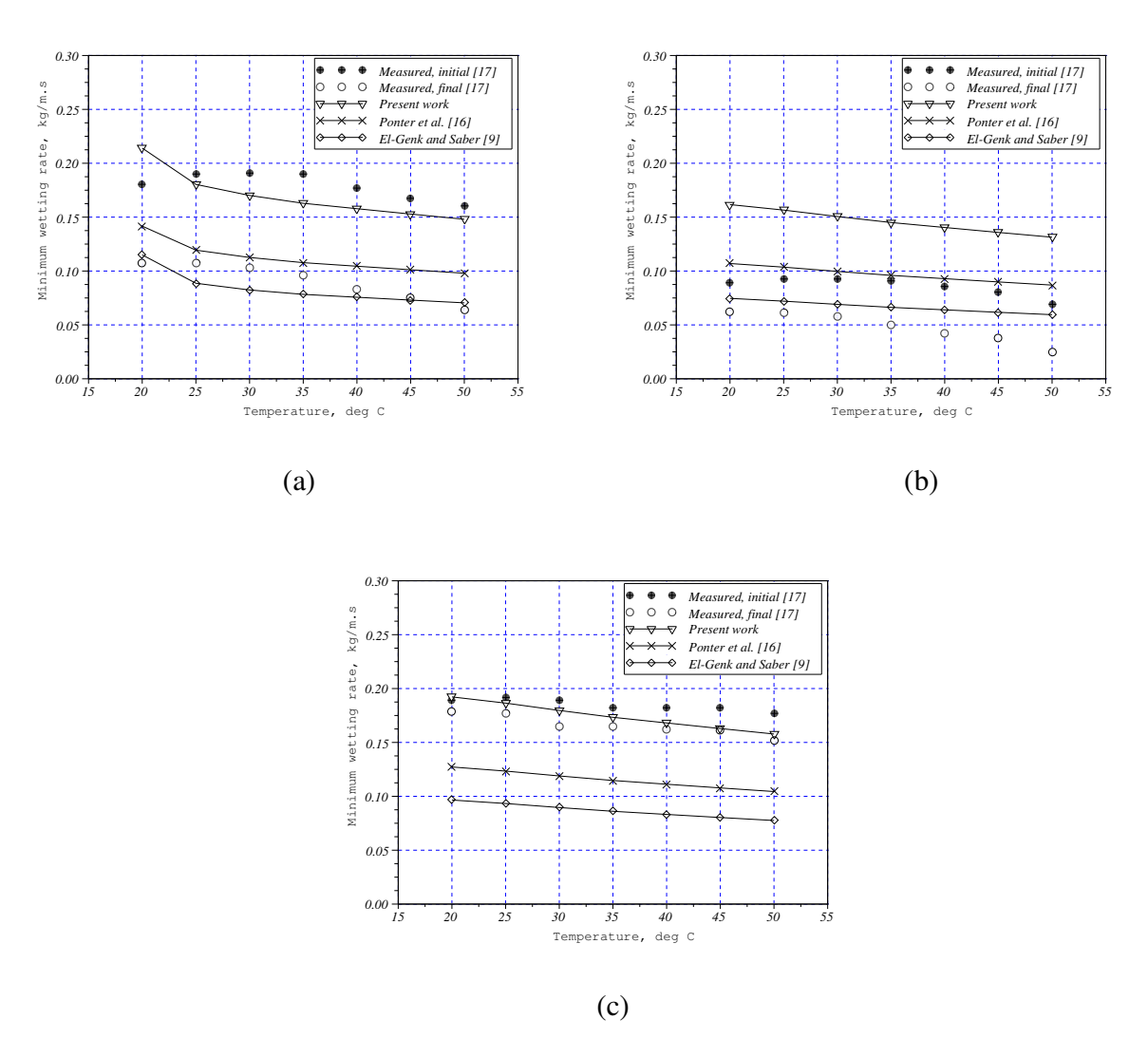


Fig. 3. Predictions of the minimum wetting rate of liquid film flowing down (a) copper surface, (b) stainless steel surface, (c) Perspex surface. Contact angle data taken from [16], [17].

As shown in the figure, the present predictions are in good agreement with the measured data. For the copper and the Perspex surfaces the predicted minimum wetting rate of the liquid film stays between the measured initial and final wetting rates, while for the stainless steel surface the predicted minimum wetting rate is higher than both these values. It should be noted that in all calculations an equilibrium static contact angle was used. A certain discrepancy between measurements and predictions is observed for low temperatures, in the range from 20 to 30 °C, where the measured minimum wetting rate stays constant or slightly increases with increasing temperature. All presented models predict a decreasing minimum wetting rate in the whole temperature range. This is due to the fact that the contact angle linearly decreases with increasing temperature at a rate of -0.1°/°C, [16]. The reason why the measured minimum wetting rate stays constant or increases with temperature in the range from 20 to 30 °C is unknown.

Hewitt and Lacey [11] measured the minimum wetting rate of a climbing liquid film for adiabatic air-water annular two-phase flow in a vertical 12.7mm/31.75mm annulus. The dry patch was created artificially by blowing air on the wall covered with the liquid film. Consecutively the flow rate of the

liquid film was decreased until the dry patch could not be rewetted. Hewitt and Lacey [11] compared the measurements with own calculations based on the model by Hartley and Murgatroyd [12] and concluded that the predictions in general gave much higher values of the minimum wetting rate as observed in the measurements. The predictions could be matched with the measurements only if the contact angle was assumed to be equal to 17° in the calculations. That was much lower value than the static contact angle of 46° measured by the same authors for relevant conditions. Hewitt and Lacey suggested that the discrepancy between the predictions and measurements could be due to the fact that the model was lacking of an aerodynamic force acting on the leading edge of the liquid film. Another explanation could be that the Hartley and Murgatroyd's model assumes laminar flow in the liquid film, whereas the flow was turbulent in the experiments.

Comparison of the present model given by Eq. (34a) with Hewitt and Lacey data is shown in Fig. 4. As can be seen, the experimental data can be matched by the predictions when the contact angle is assumed equal to 24.5°. Increasing the contact angle to 30° gives the minimum wetting rate which is higher than the measured one by approximately 50%. In spite of this discrepancy, the model correctly predicts decreasing minimum liquid flow rate with increasing air flow rate. In that respect, the present results are consistent with the results reported by Hewitt and Lacey. However, due to inclusion of the shape and skin drag forces acting on the leading edge of the liquid film, some improvement can be noticed. The present results indicate that the contact angle plays important role in the over-all accuracy of the model. Since the local value of the contact angle is influenced by several factors, such as for example temperature, future formulation of the model should be extended to include heat transfer effects, taking into account the precursory cooling and employing the conjugate heat transfer approach.

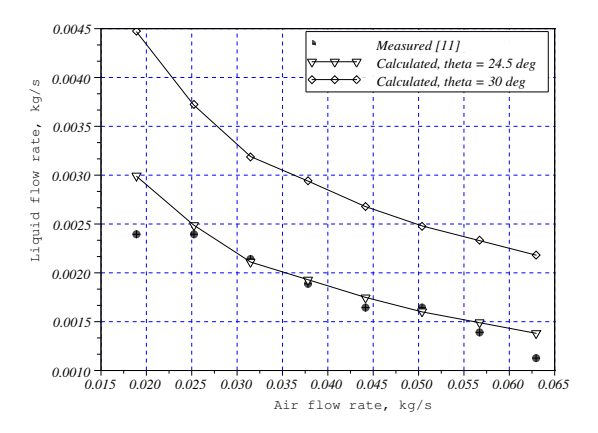


Fig. 4. Minimum liquid film flow rate as a function of air flow rate. Comparison of predictions with experimental data [11].

Since the results shown in Fig. 4 have been obtained by employing the laminar film flow model, a relevant question is whether such approximation is admissible for the present conditions. To investigate the influence of turbulence on results of predictions, various turbulence models were employed. Figures 5(a-c) show the velocity profiles, minimum re-wetting liquid film Reynolds number and the relative stagnation force (a ratio of the stagnation force to the surface tension force) obtained with the laminar and the three turbulence models described in Section 1.1.

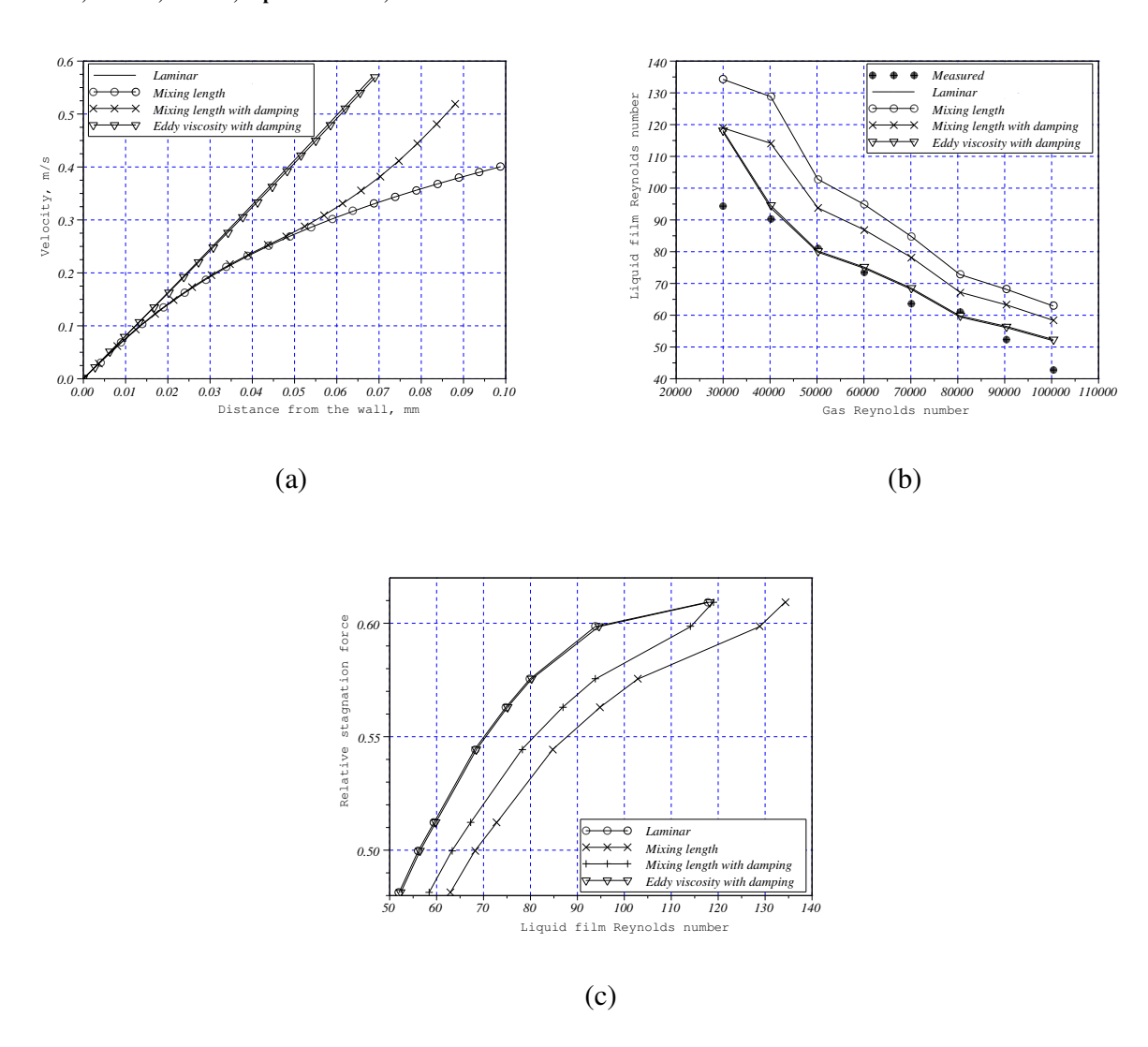


Fig. 5. Influence of turbulence models on dry patch re-wetting in air-water annular flow in 12.7mm/31.75mm annulus at atmospheric pressure and contact angle 24.5°: (a) velocity profiles in liquid film, (b) minimum re-wetting liquid film Reynolds number as a function of gas Reynolds number, (c) ratio of stagnation force to surface tension force as a function of liquid film Reynolds number.

Figure 5(a) indicates that the velocity profiles for laminar flow as well as for turbulent flow using the viscosity model given by Blanghetti and Schlunder [15] are similar. The mixing length and the modified mixing length models predict more flat velocity distributions due to a higher value of the turbulent viscosity. As a result, the liquid film thickness increases, when the total mass flow rate is kept constant. Figure 5(b) shows that the minimum film Reynolds number, corresponding to the minimum wetting rate, predicted with the laminar flow assumption is very close to the results obtained with the Blanghetti and Schlunder [15] turbulence model. At the same time, the mixing length and the modified mixing length models yield higher values of the minimum film Reynolds number. This leads to a conclusion that the discrepancy between measurements and predictions for the Hewitt and Lacey data is not caused by the neglect of turbulence in the liquid film, since the increasing level of turbulence shifts the predicted minimum film Reynolds number (and thus the minimum re-wetting rate) further away from the measured values. Figure 5(c) shows the magnitude

of the relative stagnation force, defined as a ratio of the stagnation force to the surface tension force, as a function of the liquid film Reynolds number. As expected, this force increases with increasing film Reynolds number. It can also be seen that for turbulent films, this force decreases, while keeping the film Reynolds number constant. This is due to the increasing thickness and the decreasing flow velocity in liquid films with the increasing level of turbulence.

4. Conclusion

An analysis is presented that predicts the conditions which allow for a formation of a stable dry patch in diabatic annular two phase flows. The analysis employs a force balance formulated for the leading edge of the liquid film. In addition to stagnation, thermo-capillary and vapor thrust forces, the analysis includes effects of the pressure gradient and the interfacial shear stress. The importance of turbulence in the liquid film is investigated by comparing results obtained with various turbulence models to the analytical solution valid for laminar flow as well as to selected experimental data.

It is concluded that the present model gives results which are in good agreement with experiments and analytical expressions given by Ponter et al. [16] and El-Genk and Saber [9] in case of an isothermal liquid film flowing down a vertical surface. For adiabatic annular two-phase flow, the data obtained by Hewitt and Lacey [11] were used as a reference. The model correctly predicts a decreasing minimum wetting rate of a dry patch with increasing flow rate of the gas phase. The measured wetting rate could be matched with using the contact angle that was equal to a half of the static contact angle reported in the experiments.

The analyses performed for steam-water mixtures at various pressures indicate that the dominant forces which govern the dry patch stability are due to the stagnation pressure and the surface tension effects. In absence of other forces, the minimum wetting rate is governed by the balance between these two forces. With increasing heat flux, the importance of the thermo-capillary force grows and its neglect may lead to a significant error. The fourth important force is due to the skin friction. Its magnitude can be comparable to the stagnation force for small contact angles. This effect increases with increasing pressure of the two-phase mixture.

The present results indicate that the contact angle plays important role in the over-all accuracy of the model. Since the local value of the contact angle is influenced by several factors, such as for example temperature, future formulation of the model should be extended to include heat transfer effects, taking into account the precursory cooling and employing the conjugate heat transfer approach.

5. References

- [1] G.F. Hewitt and A.H. Govan, "Phenomenological modeling of non-equilibrium flows with phase change", *Int. J. Heat Mass Transfer*, Vol. 33, No. 2, 1990, pp. 229-242.
- [2] C. Adamsson and H. Anglart, "Influence of axial power distribution on dryout: Film flow models and experiments", *Nuclear Engineering and Design*, Vol. 240, 2010, pp. 1495-1505.
- T. Ueda and Y. Isayama, "Critical heat flux and exit film flow rate in a flow boiling system", *Int. J. Heat Mass Transfer*, Vol. 24, No. 7, 1981. pp. 1267-1276.

- [4] T. Fukano, S. Mori, T. Nakagawa, "Fluctuation characteristics of heating surface temperature near an obstacle in transient boiling two-phase flow in a vertical annular channel", *Nuclear Engineering and Design*, Vol. 219, 2003, pp. 47-60.
- [5] T. Hobler, "Minimum surface wetting", *Chemia Stosowana*, Vol. 2B, 1964, pp. 145-159.
- [6] S.G. Bankoff, "Minimum thickness of a draining liquid film", *Int. J. Heat Mass Transfer*, Vol. 14, 1971, pp. 2143-2146.
- [7] J. Mikielewicz and J.R. Moszynski, "Minimum thickness of a liquid film flowing down a solid surface", *Int. J. Heat Mass Transfer*, Vol. 19, 1976, pp. 771-776.
- [8] A. Doniec, "Laminar flow of a liquid rivulet down a vertical solid surface", *Can. J. Chem. Eng.*, Vol. 69, 1991, pp. 198-202.
- [9] M.S. El-Genk and H.H. Saber, "Minimum thickness of a flowing down liquid film on a vertical surface", *Int. J. Heat Mass Transfer*, Vol. 44, 2001, pp. 2809-2825.
- [10] J. Mikielewicz, D. Mikielewicz, S. Gumkowski, "A model of liquid film breakdown formed due to the impingement of a two-phase jet on a horizontal surface", *Int. J. Heat Mass Transfer*, Vol. 53, 2010, pp. 5456-5464.
- [11] G.F. Hewitt, P.M.C. Lacey, "The breakdown of the liquid film in annular two-phase flow", *Int. J. Heat Mass Transfer*, Vol. 8, 1965, pp. 781-791.
- [12] D.E. Hartely, W. Murgatroyd, "Criteria for the break-up of thin liquid layers flowing isothermally over solid surface", *Int. J. Heat Mass Transfer*, Vol. 7, 1964, pp. 1003-1015.
- [13] N. Zuber, F.W. Staub, "Stability of dry patches forming in liquid films flowing over heated surfaces", *Int. J. Heat Mass Transfer*, Vol. 9, 1966, pp. 897-905.
- [14] G.D. McPherson, "Axial stability of the dry patch formed in dryout of a two-phase annular flow", *Int. J. Heat Mass Transfer*, Vol. 13, 1970, pp. 1133-1152.
- [15] F. Blanghetti, E.U. Shlunder, "Local heat transfer coefficients on condensation in vertical tubes", Proc. 6th Int. Heat Transfer Conference, 2 (1978) 437-442.
- [16] B. Ponter, G.A. Davies, W. Beaton, T.K. Ross, "The measurement of contact angles under conditions of heat transfer when a liquid film breaks on a vertical surface", *Int. J. Heat Mass Transfer*, Vol. 10, 1967, pp. 1633-1636.
- [17] B. Ponter, G.A. Davies, T.K. Ross, P.G. Thornley, "The influence of mass transfer on liquid film breakdown", *Int. J. Heat Mass Transfer*, Vol. 10, 1967, pp. 349-359.